InAlN/GaN Detectors for Real-Time Dosimetry in Ultra-High Dose Rate FLASH Radiotherapy

Published in final edited form as:
IEEE Sens Lett. 2026 January ; 10(1): . doi:10.1109/lsens.2025.3636392.

InAlN/GaN Detectors for Real-Time Dosimetry in Ultra-High Dose Rate FLASH Radiotherapy

Si Young Choi[1,†], **Cierra Anderson**[1], **Kevin Dai**[2], **Ilaria Fratelli**[3], **Yi-Chen Liu**[1], **Peter Ballentine**[1], **Yuewen Tan**[4], **Michael Bardash**[5], **Guy Garty**[4], **Andrew Harken**[4], **Ioannis Kymissis**[1,**], **Savannah Eisner**[1,*]

[1] Department of Electrical Engineering, Columbia University, New York, NY 10027, USA

[2] Department of Electrical and Computer Engineering, University of Illinois at Urbana-Champaign, Urbana, IL 711103, USA

[3] Department of Physics and Astronomy, University of Bologna, Bologna 40126, Italy

[4] Radiological Research Accelerator Facility, Columbia University, New York, NY 10032, USA

[5] Radiation Detector Solutions, Albuquerque, NM 87110, USA

Abstract

This letter reports the first characterization of InAlN/GaN-on-Si solid-state detectors under ultra-high dose-per-pulse (UH-DPP) electron irradiation for FLASH radiotherapy applications. Unpassivated Ni/Au metal-semiconductor-metal (MSM) and two-dimensional electron gas (2DEG) interdigital transducer (IDT) detectors exhibited the best transient performance, with the 2DEG IDT resolving individual pulses as short as 3 μs rise and 325 μs fall times and achieving a signal-to-noise ratio (SNR) exceeding 220 under 2 Gy pulses. Across a dose-per-pulse (DPP) range of 0.05–0.5 Gy, the 2DEG IDT detector demonstrated consistent, dose-dependent voltage responses with sensitivities of 0.5–0.9 V/Gy and a normalized sensitivity of 48.75 nC/Gy/mm^2, one to two orders of magnitude higher than reported SiC and diamond detectors. These results establish InAlN/GaN detectors as promising candidates for compact, high-speed, and radiation-tolerant dosimetry systems capable of real-time single-pulse monitoring in clinical FLASH radiotherapy.

Graphical Abstract

Corresponding author: S. R. Eisner (savannah.eisner@columbia.edu). † S. Y. Choi was with the Department of Electrical Engineering, Columbia University, New York, NY 10027, USA. He is now with the Department of Electrical and Computer Engineering, North Carolina State University, Raleigh, North Carolina 27695, USA (schoi32@ncsu.edu).
*Member, IEEE
**Fellow, IEEE

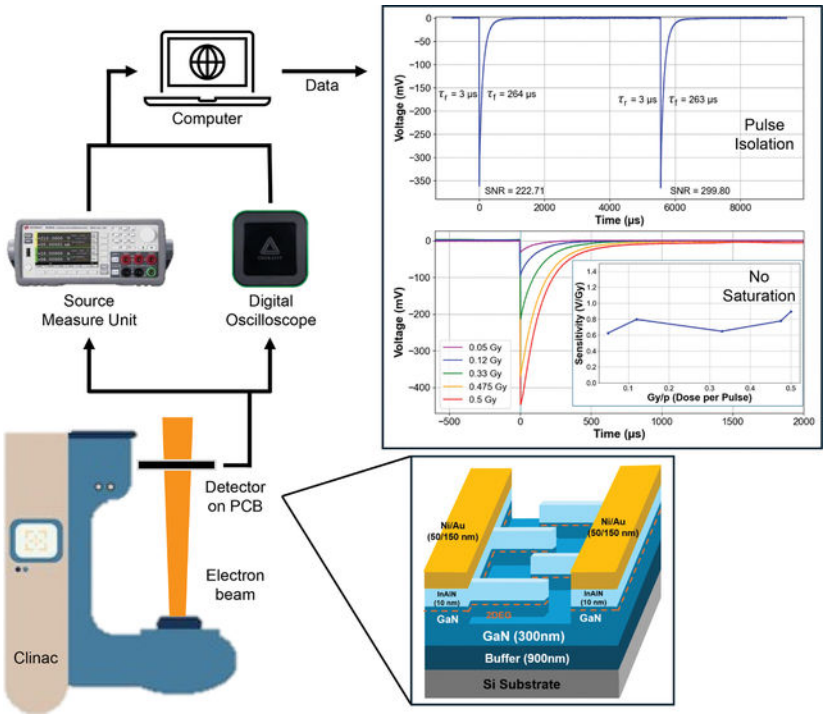

Index Terms—

dosimeter; FLASH radiotherapy; Gallium Nitride; UH-DPP; 2DEG

I. INTRODUCTION

A novel external beam radiotherapy (EBRT) technique called FLASH radiotherapy that uses ultra-high dose-rate (UHDR) of at least 40 Gy/s electron/proton/X-ray beams has been investigated for cancer treatment to minimize the radiation-induced damage in surrounding healthy tissue with fewer and shorter treatments of about 90 ms [1]. However, due to the significantly higher dose rate and shorter treatment time, FLASH radiotherapy presents challenges in dosimetry compared to conventional EBRT. Traditional techniques for dosimetry including ion chambers and radiochromic films offer limited response times and saturate high dose rates, precluding accurate in vivo transit dosimetry for safe FLASH radiotherapy [1]. In order to overcome these challenges, preliminary demonstrations of FLASH radiotherapy dosimeters have been reported [2–5]. Single pulse detection, necessary for real-time dose monitoring and in particular to allow stopping the beam when the prescribed dose has been reached, has only been demonstrated in diamond-based solid-state detectors [6, 7]. Recently, high-pressure high-temperature (HPHT)-grown diamond detectors as a cheaper alternative have shown promising performance [8], yet their fabrication and scalability remain more restrictive than those of GaN technologies, which enable detector arrays and monolithic integration.

In contrast, wide-bandgap gallium nitride (GaN) is significantly cheaper than diamond and benefits from a more mature fabrication processes [9]. GaN also exhibits high

breakdown voltage and electron saturation velocity [10], making it well-suited for high-speed detection. Paramount for EBRT applications, GaN-based devices have exhibited strong radiation tolerance in high-energy particle and photon environments, maintaining performance after exposure to total ionizing doses exceeding tens of kGy and post-irradiation I-V recovery after hundreds of kGy [11–13]. Additionally, the polarization-induced two-dimensional electron gas (2DEG) formed in GaN heterostructures enables high carrier density and mobility without the need for doping; 2DEG-based GaN devices have demonstrated excellent performance in sensing and high-frequency applications [14, 15]. While aluminum gallium nitride/gallium nitride (AlGaN/GaN) heterostructures are primarily used in GaN-based sensing applications, indium aluminum nitride/gallium nitride (InAlN/GaN) heterostructures support higher 2DEG density and carrier confinement [16]. These attributes make InAlN/GaN attractive for enhancing signal amplitude and reducing RC-limited response times, advantageous for fast, high-dose rate dosimetry [17]. In this work, we demonstrate for the first time the application of InAlN/GaN solid-state detectors for FLASH radiotherapy dosimetry, achieving individual pulse resolution with rise and fall times of 3 μs and 325 μs, respectively, and a signal-to-noise ratio exceeding 1600. These results establish InAlN/GaN-on-Si metal-semiconductor-metal (MSM) and 2DEG interdigital transducer (IDT) devices as promising candidates for high-speed, real-time monitoring of FLASH beams across clinically relevant dose rates. Importantly, the observed linear relationship between detector signal intensity and dose-per-pulse (DPP) provides a pathway for precise system calibration and feedback control.

II. FABRICATION AND MEASUREMENT

A. Device Fabrication

Detectors were fabricated on a commerically-sourced InAlN/GaN-on-Si wafer. The nitride epitaxial stack comprises a 10-nm thick $In_{0.17}Al_{0.83}N$ barrier layer, 0.8-nm thick AlN spacer, 900-nm thick Fedoped GaN strain management buffer layer, and an active 300-nm thick GaN layer grown on a 675-μm thick p-type Si substrate (Fig. 1a). Hall effect measurements indicate a two-dimensional electron gas (2DEG) sheet carrier concentration of 13.624×10^{12} cm^{-2} and a mobility of 914.5 $cm^2/V{\cdot}s$. Three key device parameters were evaluated in this work: the presence of 2DEG formed at the InAlN/GaN interface, the use of the 2DEG as an interdigitated transducer (IDT), and the deposition of an Al_2O_3 passivation layer. InAlN/GaN MSM and IDT detectors incorporating the 2DEG channel were fabricated on the mesa, with the 2DEG IDT fingers defined by chlorine-based reactive ion etching (RIE) of the InAlN barrier to a depth of approximately 90 nm. In contrast, the GaN MSM detector was realized by fully removing the InAlN barrier in the active region during the same RIE etch. Following mesa definition, Ni/Au (50/150 nm) Schottky metal was deposited as the electrodes and bond pads of the MSM devices, excluding the etched 2DEG IDT fingers. Lastly, a subset of detectors were passivated with 15-nm thick atomic layer deposited (ALD) Al_2O_3. Optical microscope images of the fabricated detectors are shown in Fig. 1(b)–(e). All finger widths and spacings are 5 μm and 3 μm, respectively. The active area of all detectors is ~4000 $μm^2$.

B. Measurement Setup

The detector die was adhered to a printed circuit board (PCB) and detector bond pads were wire bonded to PCB pads. This inner PCB was connected to an outer PCB via pin headers and sockets, which was interfaced with BNC cables via connectors for electrical measurements (Fig. 2a). Both the inner and outer PCBs were wrapped in aluminum foil to prevent electromagnetic interference. The detectors were measured in-situ using a 15 or 16 MeV electron beam generated by a modified clinical linear accelerator (Clinac 2100C, Varian Medical Systems) [18]. The Clinac was operated in 15 MV (photon) mode with the target removed to obtain a pulsed electron beam with a dose of 0.5 Gy per 5 μs pulse (instantaneous dose rate: 10^5 Gy/s; average dose rate: 90 Gy/s) or 0.36 Gy per pulse (instantaneous dose rate: 7×10^4 Gy/s; average dose rate: 65 Gy/s) or in 16 MeV (electron mode) to obtain a dose rate of 0.025 Gy per pulse (instantaneous dose rate: 5000 Gy/s; average dose rate: 4.5 Gy/s). Source to sample distance was 170 cm. The pulse rate was 180 Hz for most experiments. For a subset of experiments, a lower pulse rate of 15 Hz (0.36 Gy/pulse; 5.4 Gy/s) was used. Gun current and deQing were set as described in [19] to achieve the required dose rate. Dose rate was measured using an Advanced Markus ion chamber and Unidos E electrometer and verified using EBT3 Gafchromic film (Ashland Inc.). Readout was performed using a Keysight B2901A source measure unit (SMU) with a 1 V bias, and a Digilent Analog Discovery 3 digital oscilloscope for current sampling and voltage signals, respectively. Figure 2(b)–(c) shows the CLINAC and detector setup.

III. EXPERIMENTAL RESULTS AND DISCUSSION

The sampled current signal from the Keysight B2901A SMU over time of the Al_2O_3 Ni/Au-MSM, Ni/Au-MSM, GaN Ni/Au-MSM, and 2DEG IDT, all exposed under 360 pulses of 0.36 Gy/pulse dose (total of 129.6 Gy), is displayed in Fig. 3. The total period of irradiation was ~2 seconds. This cumulative irradiation sequence not only allowed the evaluation of the detector response over a clinically relevant total dose rate, but also served as an initial indicator of radiation hardness, as all devices maintained functionality throughout extended exposure. Rise and fall times were defined as the time intervals between 10% and 90% of the signal maximum and vice versa (Table 1). Unpassivated and Al_2O_3-passivated Ni/Au-MSMs were compared first. The rise time of the unpassivated Ni/Au-MSM shown in Fig. 3 and Table 1 was the shortest, at τ_r= 0.89 s. This discrepancy is attributed to charge accumulation in the Al_2O_3 passivation layer and charge trapping at the dielectric-semiconductor interface. Interface traps can occur due to fabrication defects introduced during ALD, such as oxygen vacancies and dangling bonds, as well as lattice mismatch at the border. These features capture and release carriers, leading to a higher threshold voltage and therefore a slower RC response [20]. Due to this significantly faster fall time without passivation, unpassivated GaN Ni/Au-MSM and 2DEG IDT devices were chosen to expose under the electron beam as well. Both the GaN Ni/Au-MSM and 2DEG IDT detectors exhibited a lower total sampled current compared to the InAlN Ni/Au-MSM devices, despite having the same active area. The lower current in the 2DEG IDT is attributed to a slight lateral misalignment (25 μm) between the mesa and the MSM layers, resulting in asymmetric contacts as seen in Fig. 1(d). A lower current is expected in the GaN MSM as a result of its much lower carrier density. The longer apparent fall time in cumulative signals

likely arises from charge trapping during repeated pulses; individual pulse response remains symmetric and fast (~3 μs).

Due to its superior fall time, the unpassivated 2DEG IDT detector was selected for high-speed pulse-resolution measurements with a Digilent digital oscilloscope. As shown in Figure 4, the detector successfully resolved two consecutive 2 Gy pulses, with a minimal voltage variation of 4 mV. Each pulse was detected within 3 μs with a signal-to-noise ratio (SNR) of an average of 261. The signal decayed back to baseline within 300 μs, well before the arrival of the next pulse in a period of 5.5 ms, corresponding to an effective pulse width of ~300 μs. These results demonstrate that the 2DEG IDT can reliably detect individual pulses with high temporal resolution and rapid recovery, making it a strong candidate for real-time dosimetry tasks such as active gate beaming or precise dose cut-off during treatments, a critical requirement for safe administration of FLASH radiotherapy. Fig. 5 presents the individual pulse voltage signals and sensitivities of the unpassivated 2DEG IDT when exposed to different DPP levels, with summarized metrics in Table 2. The detector consistently resolved each pulse across the tested range (0.05–0.5 Gy/pulse), with rise times remaining within a few microseconds and fall times below 350 μs. The inset highlights the calculated sensitivity (V/Gy) based on the peak voltage of each pulse, showing no saturation effects. The nearly linear increase in peak signal with dose confirms that the detector output is directly proportional to absorbed DPP, establishing a pathway for converting measured voltage signals to absolute dose. Fig. 6 further illustrates the clear correlation between voltage signal intensity and DPP. The unpassivated 2DEG IDT demonstrates consistent, dose-dependent voltage responses across varying DPP levels, with sensitivity ranging from 0.5 to 0.9 V/Gy. The voltage variation in Fig. 4 and the nonlinear response in Fig. 6 likely arise from transient charge trapping and RC limitations in the readout circuit, compounded by undersampling of fast transients at the 800 kHz acquisition rate. Future work will employ higher-bandwidth readout and extended pulse trains to further quantify and mitigate these effects.For comparison with existing technologies, Table 3 tabulates the time to 99.5% charge collection, DPP sensitivity, and active area of this work compared to previously reported state-of-the-art silicon carbide (SiC) and diamond detectors for FLASH dosimetry. The InAlN/GaN 2DEG IDT achieved the fastest rise time, outperforming both SiC and diamond. Although the absolute sensitivity of the SiC detector (~450 nC/Gy) is higher, it requires a much larger active area (100 mm^2), resulting in a relatively low normalized sensitivity of ~4.5 nC/Gy/mm^2. In contrast, the 2DEG IDT demonstrates a compact active area of only 0.004 mm^2 with a normalized sensitivity of 870.66 nC/Gy/mm^2, nearly three orders of magnitude greater than SiC and an order of magnitude higher than diamond. This highlights the exceptional efficiency of the InAlN/GaN platform when scaled down to small detector footprints, a critical attribute for integration into high-density arrays or minimally invasive in vivo probes.

IV. CONCLUSION

In summary, InAlN/GaN-on-Si MSM and IDT detectors demonstrated high-speed performance under FLASH-relevant irradiation, with the unpassivated 2DEG IDT achieving the fastest response and reliable single-pulse detection. A clear correlation between signal intensity and dose-per-pulse was established, enabling straightforward calibration. These

results highlight the promise of GaN-based wide bandgap devices as compact, low-cost candidates for real-time FLASH dosimetry. Future work will investigate charge trapping effects under cumulative irradiation to further elucidate the observed slow decay in sampled signals and focus on improving linearity, extending to higher dose-per-pulse regimes, and assessing long-term radiation hardness.

ACKNOWLEDGMENT

We acknowledge the use of facilities and instrumentation supported by NSF through the Columbia University, Columbia Nano Initiative, and the Materials Research Science and Engineering Center DMR-2011738. Development of the RARAF FLASH irradiator was partially supported by Grant No. U19-AI067773 from the National Institute of Allergy and Infectious Diseases (NIAID), National Institutes of Health (NIH). The Clinac was a gift from Weill Cornell Medicine, initiated by Dr Silvia Formenti, with additional support from the Radiation Oncology departments at Weill Cornell Medicine and Columbia University Irving Medical Center (Dr Lisa Kachnic), as well as an unrestricted research gift from Barry Neustein. I.F. received funding from the European Union's Horizon Europe research and innovation program under the Marie Skłodowska-Curie Actions grant agreement No 101105245. P. B. was supported by a National Science Foundation Graduate Research Fellowship under Grant No. DGE-2036197.

REFERENCES

[1]. Siddque S, Ruda HE, Chow JCL, "FLASH radiotherapy and the use of radiation dosimeters," Cancers, vol. 15, no. 15, Jul. 2023.

[2]. Romano F et al. , "First characterization of novel silicon carbide detectors with ultra-high dose rate electron beams for FLASH radiotherapy," Appl. Sci, vol. 13, no. 5, Feb. 2023.

[3]. Oh K, Hyun M, Gallagher K, Zhou S, "Characterization of a commercial plastic scintillator for electron FLASH dosimetry," Appl. Clin. Med. Phys, vol. 25, no. 8, Jul. 2024.

[4]. Kranzer R et al. , "Response of diamond detectors in ultra-high dose-per-pulse electron beams for dosimetry at FLASH radiotherapy," Phys. Med. Biol, vol. 67, no. 7, Mar. 2022.

[5]. Marinelli M et al. , "Design, realization, and characterization of a novel diamond detector prototype for FLASH radiotherapy dosimetry," Med. Phys, vol. 49, no. 3, Jan. 2022.

[6]. Pettinato S, Felici G, Galluzzo L, Rossi MC, Girolami M, Salvatori S, "A readout system for highly sensitive diamond detectors for FLASH dosimetry," Phys. and Imag. in Rad. Oncology, vol. 29, Jan. 2024.

[7]. Pettinato S, Salvatori S, "Diamond-based detection systems for tomorrow's precision dosimetry," Nuclear Inst. Met. in Phys. Research, vol. 1059, Feb. 2024.

[8]. Pettinato S, Sinisi G, Girolami M, Rossi MC, and Salvatori S, "A high performance detector based on HPHT-diamond for dosimetry of ultrahigh dose-rate electron beams," IEEE Sens. Lett, vol. 9, no. 8, Jan. 2025.

[9]. Liu A et al. , "The evolution of manufacturing technology for GaN electronic devices," Micromachines, vol. 12, no. 7, Jun. 2021.

[10]. Chaudhary OS, Denaï M, Refaat SS, Pissanidis G, "Technology and applications of wide bandgap semiconductor materials: current state and future trends," Energies, vol. 16, no. 18, Sept. 2023.

[11]. Vilas Bôas AC et al. , "Ionizing radiation hardness tests of GaN HEMTs for harsh environments," Microelectronics Reliability, vol. 116, p. 114000, Nov. 2020.

[12]. Ahn K et al. , "Differences in electrical responses and recovery of GaN p+n diodes on sapphire and freestanding GaN subjected to high dose 60Co gamma-ray irradiation," Journal of Applied Physics, vol. 129, no. 24, Jun. 2021.

[13]. Luo B et al. , "Influence of ^{60}Co γ-rays on dc performance of AlGaN/GaN high electron mobility transistors," Applied Physics Letters, vol. 80, no. 4, pp. 604–606, Jan. 2002.

[14]. Satterthwaite PF, Yalamarthy AS, Scandrette NA, Newaz AKM, and Senesky DG, "High responsivity, low dark current ultraviolet photodetectors based on two-dimensional electron gas interdigitated transducers," ACS Photonics, vol. 5, no. 11, pp. 4277–4282, Oct. 2018.

[15]. Hwang JH, Lee K, Hong S, Jang J, “Balanced MSM-2DEG varactors based on AlGaN/GaN heterostructure with cutoff frequency of 1.54 THz,” IEEE Elec. Dev. Lett, vol. 38, no. 1, Jan. 2017.

[16]. Kuzmík J, “Power electronics on InAlN/(In)GaN: Prospect for a record performance,” IEEE Elec. Dev. Lett, vol. 22, no. 11, Nov. 2001.

[17]. Kumar S, Pratiyush AS, Dolmanan SB, Tripathy S, Muralidharan R, Nath DN, “UV detector based on InAlN/GaN-on-Si HEMT stack with photo-to-dark current ratio > 10^7,” Appl. Phys. Lett, vol. 111, Art. no. 251103, Dec. 2017.

[18]. Garty G et al. , “Ultra-high dose rate FLASH irradiator at the radiological research accelerator facility,” Scientific Reports, vol. 12, no. 1, Dec. 2022.

[19]. Tan Y, Deoli NT, Harken AD, Brenner DJ and Garty G, “Beam intensity and stability control on a modified clinical linear accelerator for FLASH irradiation.” Phys. Med. Biol, vol. 70, no.16 2025.

[20]. Kumar S et al. , “Interface traps at Al2O3/InAlN/GaN MOS-HEMT -on- 200 mm Si,” Solid-State Electronics, vol. 137, pp. 117–122, Sep. 2017.

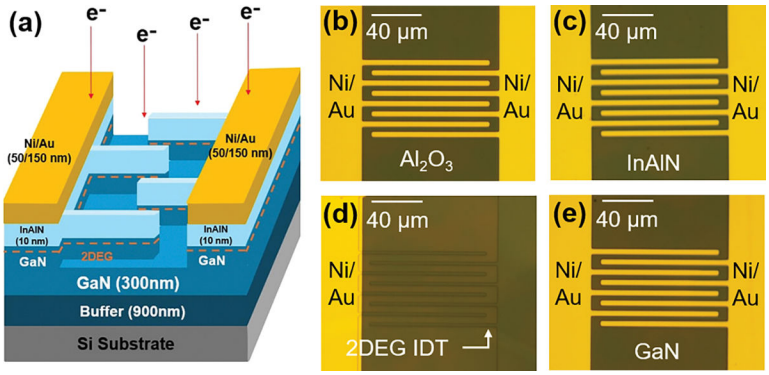

Fig. 1.

(a) Schematic of the InAlN/GaN two-dimensional electron gas (2DEG) interdigital transducer (IDT) detector shown in (d). Top view optical microscope images of the microfabricated (b) Al_2O_3-passivated InAlN/GaN Ni/Au metal-semiconductor-metal (MSM) detector, (c) unpassivated InAlN/GaN Ni/Au MSM detector, (d) InAlN/GaN 2DEG IDT detector and (e) GaN Ni/Au MSM detector.

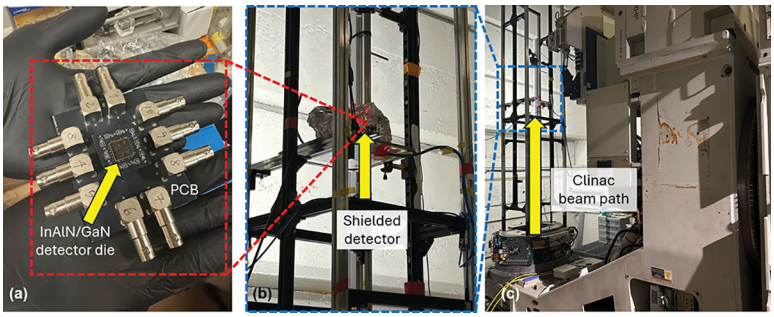

Fig. 2.

Experimental test setup for FLASH irradiation of InAlN/GaN detectors. (a) Detector die packaged on PCB. (b) Shielded detector assembly mounted on an aluminum frame, positioned at the irradiation site. (c) Modified Clinac with arrow indicating the detector placement relative to the beam path.

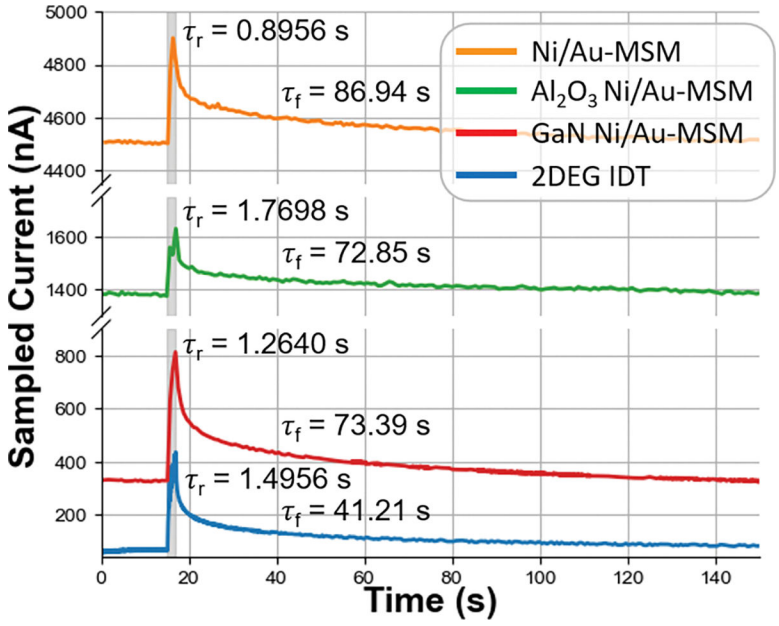

Fig. 3.

Sampled current signals over time of the demonstrated Ni/Au-MSM, Al_2O_3 Ni/Au-MSM, GaN Ni/Au-MSM, and 2DEG IDT detectors with annotated rise and fall times. Gray shaded regions indicate when the electron beam was on for a total dose of 129.6 Gy.

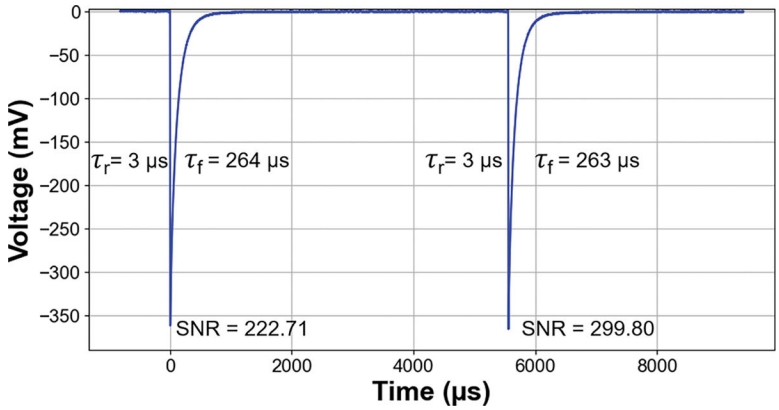

Fig. 4.

Voltage response over time of the demonstrated unpassivated InAlN/GaN 2DEG IDT detector under two consecutive 2 Gy pulses with rise time, fall time, and SNR annotated.

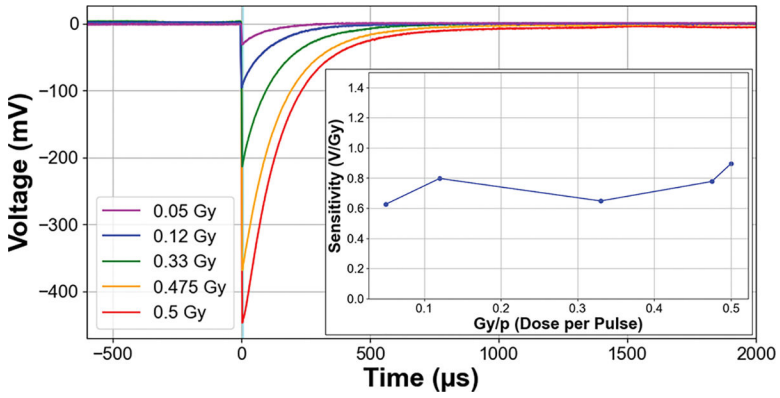

Fig. 5.

Voltage response over time of the demonstrated unpassivated InAlN/GaN 2DEG IDT exposed under varying dose-per-pulse (DPP). The inset shows the sensitivity (V/Gy) calculated from the peak voltage signal of the 2DEG IDT across varying DPP.

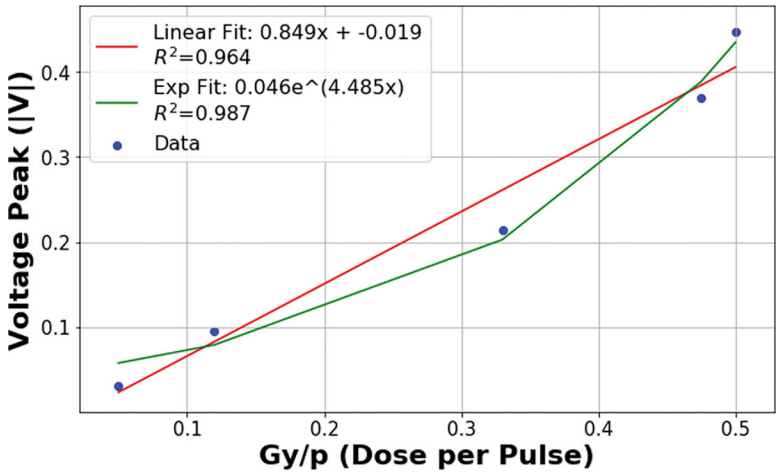

Fig. 6.

Voltage signal peaks of the InAlN/GaN 2DEG IDT detector DPP ranging from 0.05 Gy/pulse to 0.5 Gy/pulse with linear fit.

TABLE 1.

Rise and fall times (τ_r, τ_f) of fabricated GaN-based detectors under FLASH-relevant 15 MeV electron beam irradiation for a total dose of 129.6 Gy for 2 seconds.

Detector	τ_r (s)	τ_f (s)
InAlN/GaN Ni/Au-MSM	0.89	86.94
Al_2O_3 InAlN/GaN Ni/Au-MSM	1.76	72.85
GaN Ni/Au-MSM	1.26	73.39
InAlN/GaN 2DEG IDT	1.49	41.21

TABLE 2.

Rise time, fall time, and signal-to-noise ratio (SNR) of the InAlN/GaN 2DEG IDT from 0.05 Gy/pulse to 0.5 Gy/pulse.

Absorbed Dose (Gy/pulse)	τ_r (μs)	τ_f (μs)	SNR
0.05	2	205	70.84
0.12	3	255	134.71
0.33	3	289	361.90
0.475	3	324	529.64
0.5	3	325	1606.15

TABLE 3.

Comparison of rise time to 99.5% of peak charge, sensitivity, and active areas of 2DEG IDT and reference detectors

Detector	τ_r (μs)	Sens. (nC/Gy)	Active Area (mm^2)	Sens./Active Area ($nC/Gy/mm^2$)
InAlN/GaN 2DEG IDT (This work)	**1.55**	**3.483**	**0.004**	**870.66**
SiC [3]	-	~450	100	~4.5
Diamond [10]	-	25.16	0.8	31.45